The Astrophysical Journal Letters, 738:L16 (5pp), 2011 September 1 doi:10.1088/2041-8205/738/1/L16

THE DUST ENVIRONMENT OF MAIN-BELT COMET P/2010 R2 (LA SAGRA)

F. Moreno[1], L. M. Lara[1], J. Licandro[2,3], J. L. Ortiz[1], J. de León[1], V. Alí-Lagoa[2,3], B. Agís-González[2,3], and A. Molina[1,4]
[1] Instituto de Astrofísica de Andalucía, CSIC, Glorieta de la Astronomía s/n, 18008 Granada, Spain; fernando@iaa.es
[2] Instituto de Astrofísica de Canarias, c/Vía Láctea s/n, 38200 La Laguna, Tenerife, Spain
[3] Departamento de Astrofísica, Universidad de La Laguna, E-38205 La Laguna, Tenerife, Spain
[4] Departamento de Física Aplicada, Universidad de Granada, Fuentenueva s/n, 18071 Granada, Spain
Received 2011 July 13; accepted 2011 August 1; published 2011 August 16

ABSTRACT

We present a model of the dust environment of Main-Belt Comet P/2010 R2 (La Sagra) from images acquired during the period 2010 October–2011 January. The tails are best simulated by anisotropic ejection models, with emission concentrated near the nucleus south pole, the spin axis having an obliquity near 90°, indicative of a possible seasonally driven behavior. The dust mass loss rate increases rapidly shortly before perihelion, reaching a maximum value of ∼4 kg s^{-1}, and maintaining a sustained, cometary-like, activity of about 3–4 kg s^{-1} up to at least 200 days after perihelion, the date of the latest observation. The size distribution function is characterized by particles in the 5×10^{-4} cm to 1 cm radius range, assuming a time-constant power-law distribution with an index of −3.5. The ejection velocities are compatible with water-ice sublimation activity at the heliocentric distance of 2.7 AU, with values of 10–20 cm s^{-1} for particle radius of 1 cm, and inverse square root dependence on particle size, typical of hydrodynamical gas drag.

Key words: comets: individual (P/2010 R2 (La Sagra)) – methods: numerical – minor planets, asteroids: general

Online-only material: color figures

1. INTRODUCTION

Main-Belt Comet (MBC) P/2010 R2 (La Sagra) (hereafter P/La Sagra) was discovered by Nomen et al. (2010) at the La Sagra Observatory in Spain on 2010 September 14.9 UT, using a 0.45 m $f/2.8$ reflector, as a result of a long-term sky survey. The object showed some diffuse structure, being identified as an MBC, the sixth object falling in this category (Hsieh & Jewitt 2006). MBCs have dynamical properties of asteroids (i.e., Tisserand parameters with respect to Jupiter larger than three), but physical characteristics of comets (gas and/or dust emission). A review of the MBCs discovered to date is given by Bertini (2011). The MBCs discovered so far are dynamically stable, located on the orbital parameter space far enough from resonance regions, suggesting that they are native members of the Main Asteroid Belt, and not recently captured objects from elsewhere (Hsieh et al. 2009). The most recent MBC discovered, and most distinct due to its large size (110 km in diameter), is asteroid (596) Scheila (Larson 2010), which experienced a sudden outburst which has been linked to a collision with another main-belt asteroid (Bodewits et al. 2011; Jewitt et al. 2011; Moreno et al. 2011).

In this Letter we report on images of P/La Sagra at different dates, and make an interpretation of the variation of tail morphology and brightness with time using a forward Monte Carlo dust tail model, in order to provide estimates of the dust loss rates as a function of time, character of the emission (anisotropy), particle ejection velocities, and size distribution function.

2. OBSERVATIONS AND DATA REDUCTION

Images of P/La Sagra were obtained at several dates since 2010 October 10, until 2011 January 9, using various instruments at different telescopes. Thus, the Device Optimized for the LOw RESolution (DOLORES) instrument was used at the 3.6 m Telescopio Nazionale Galileo (TNG) on 2010 October 10 and 2011 January 8–9, the Andalucia Faint Object Spectrograph and Camera (ALFOSC) at the Nordic Optical Telescope (NOT) on 2010 October 16, and the Auxiliary camera-spectrograph (ACAM) at the William Herschel 4.2 m Telescope (WHT) on 2010 October 26–28, all located at the Observatorio del Roque de los Muchachos in the island of La Palma, as well as the Calar Alto Faint Object Spectrograph (CAFOS) at the 2.2 m telescope of Calar Alto Observatory, Spain, on 2010 November 4. Variations in tail morphology during consecutive observing nights were not detected, so we selected a subset of the available observations from the extensive data set to perform the model interpretation. Table 1 shows the journal of the selected observations, along with useful information. Except for the observations with ACAM, for which a Sloan r filter was employed, Johnson R filters were used, in order to minimize possible gas emission contamination. For each observing night shown in Table 1, the median of the available images was computed in order to improve the signal-to-noise ratio. Reduction was performed using standard techniques, including bias subtraction, flat fielding, and flux calibration using zero points derived from field stars and the USNO-B1.0 catalog (Monet et al. 2003), which provides a photometric accuracy of ∼0.3 mag. The images were finally converted to solar disk intensity units appropriate for the analysis in terms of dust tail models.

Figure 1 depicts combined images of P/La Sagra acquired with the above mentioned instrumentation, at the dates shown in Table 1. The images have been all oriented to the (N, M) coordinate system (Finson & Probstein 1968). These images show remarkable activity during the whole three-month period of observations. The Earth crossed the MBC orbital plane between 2010 November 4 and 2011 January 9, and that is why we see the tail oriented toward $-N$ in the November observation and in the $+N$ direction in January. The excess brightness in the $(+N, -M)$ quadrant in the 2011 January image is just an

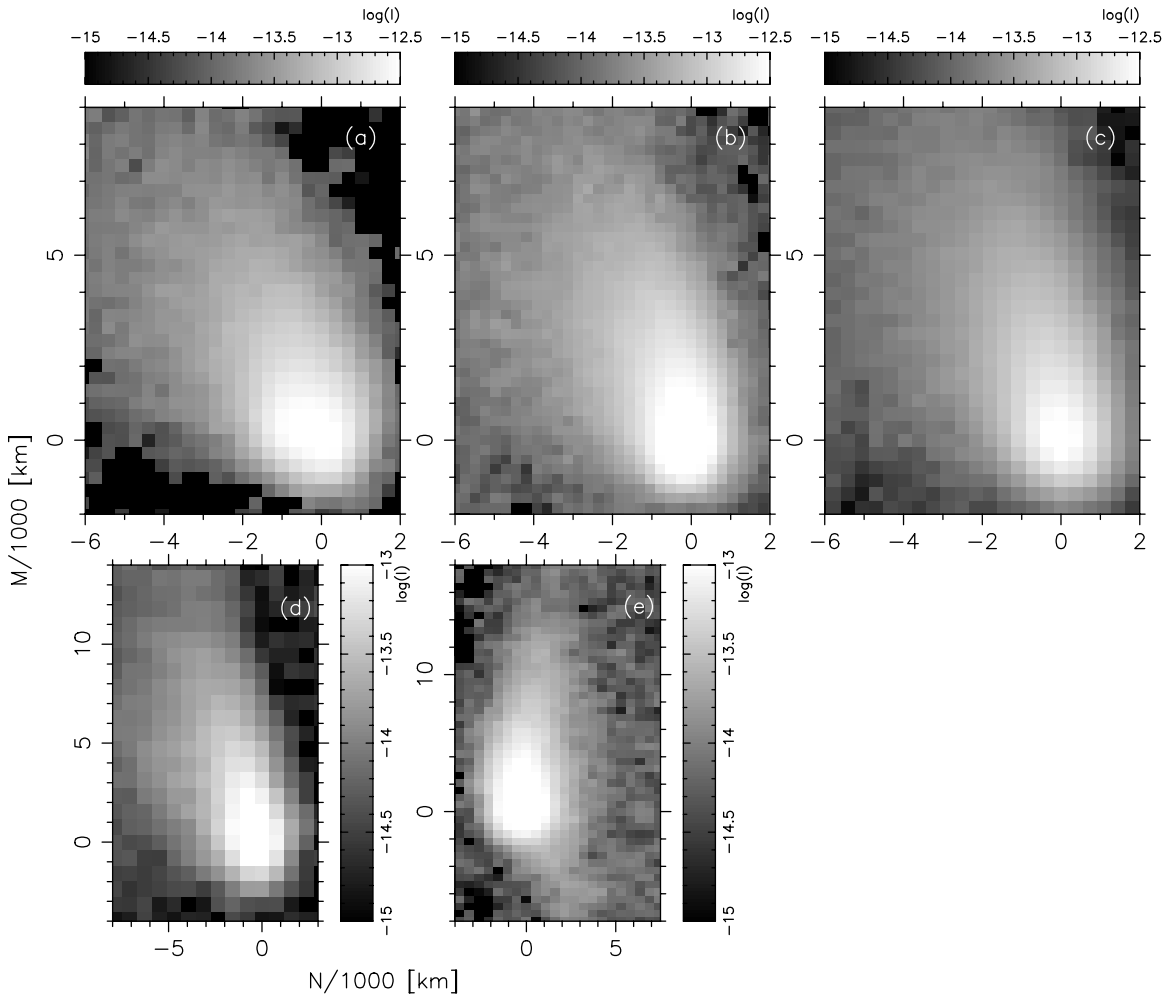

Figure 1. Images of P/La Sagra corresponding to 2010 October 10.9 (a), 2010 October 16.0 (b), 2010 October 26.9 (c), 2010 November 4.8 (d), and 2011 January 9.8 (e). Brightness is displayed in logarithmic scale, in solar disk intensity units. The images are oriented to the (N, M) coordinate system, with the scale in thousands of kilometers.

Table 1
Observational Circumstances of P/2010 R2 (La Sagra)

UT Date	Instrument/Telescope	R (AU)	Δ (AU)	α (°)	Pixel Size (km)
2010 Oct 10.9	DOLORES/TNG 3.6 m	2.660	1.860	15.3	337
2010 Oct 16.0	ALFOSC/NOT 2.5 m	2.663	1.895	16.2	261
2010 Oct 26.9	ACAM/WHT 4.2 m	2.671	1.989	18.0	361
2010 Nov 4.8	CAFOS/CAHA 2.2 m	2.680	2.080	19.3	784
2011 Jan 9.8	DOLORES/TNG 3.6 m	2.743	2.910	19.8	527

Notes. Position data include heliocentric distance R, geocentric distance Δ, and phase angle α. The pixel size refers to the spatial resolution of the images used in the model analysis.

evidence that the activity must have started near perihelion or earlier, as derived from simple synchrone analysis and confirmed by the dust model in the next sections.

3. THE MODEL

We have performed an analysis of the five images described in Table 1, and shown in Figure 1, by a direct Monte Carlo dust tail model, which is based on previous works of cometary dust tail analysis (e.g., Moreno 2009; Moreno et al. 2010), and in the characterization of the dust environment of comet 67P/Churyumov-Gerasimenko before Rosetta's arrival in 2014 (the so-called Granada model; see Fulle et al. 2010). Briefly, the code computes the trajectory of a large number of particles ejected from a cometary nucleus surface, which are exposed to solar gravity and radiation pressure. The gravity of the comet itself is neglected, which is a good approximation for small-sized nuclei (most comets are kilometer size at most). The particles are accelerated by gas drag from ice sublimation to their terminal velocities, which are the input velocities considered in the model. The particles describe a Keplerian trajectory around the Sun, whose orbital elements are computed from the terminal velocity and the ratio of the force exerted by the solar radiation pressure and the solar gravity (β; see Fulle 1989).

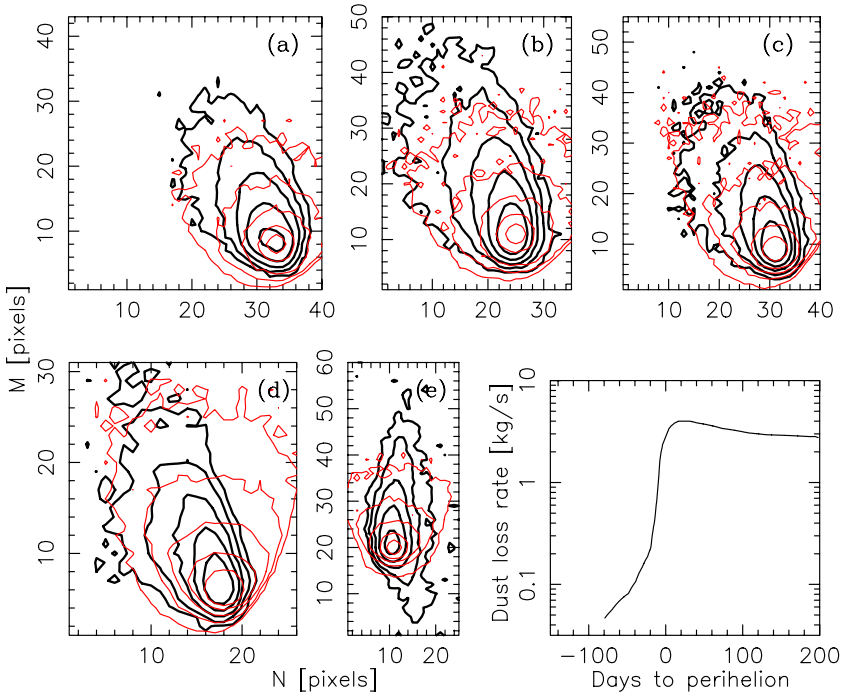

Figure 2. (a)–(e) In black thick solid lines contour plots corresponding to the observations, and in thin red lines to the isotropic model, for the following dates (UT): (a) 2010 October 10.9; (b) 2010 October 16.0; (c) 2010 October 26.9; (d) 2010 November 4.8; (e) 2011 January 9.8. Isophotes vary in factors of two, being the innermost contour of 2×10^{-14} for panels (a) and (b), 10^{-14} for panel (c), 5×10^{-15} for panel (d), and 10^{-14} for panel (e), all expressed in solar disk intensity units. The rightmost lower panel shows the variation of the dust loss mass rate with time relative to perihelion.

(A color version of this figure is available in the online journal.)

This parameter can be expressed as $\beta = C_{\rm pr} Q_{\rm pr}/(2\rho r)$, where $C_{\rm pr} = 1.19 \times 10^{-3}$ kg m^{-2} and ρ is the particle density. For particle radii $r > 0.25\,\mu$m, the radiation pressure coefficient is $Q_{\rm pr} \sim 1$ (Burns et al. 1979). For each observation date, the trajectories of a large number of dust particles are computed, and their positions on the (N, M) plane calculated. Then, their contribution to the tail brightness is computed.

4. RESULTS AND DISCUSSION

The synthetic tail brightness obtained at each date depends on the ejection velocity law assumed, the particle size distribution, the dust mass loss rate, and the geometric albedo of the particles, apart from the characteristics of the emission (anisotropy). In order to simplify the model as much as possible, we fixed some parameters to a specific value, considering previous results and our own experimentation with the model when applied to other comets. Thus, the geometric albedo was set to $p_v = 0.04$, i.e., a Halley-like value. The size distribution was assumed to be described by a time-independent power law with index -3.5. This value is within the range of previous findings in a number of comets (see, e.g., Jockers 1997 and references therein). The particles were assumed initially to vary broadly in size, from the submicrometer range up to 1 cm, and having a density of 1000 kg m^{-3}. With this parameter set, we still need to set the dust loss rate as a function of time, the velocity law, and the characteristics of the emission. We begin by assuming isotropic ejection. The particle velocity is parameterized as $v(t, \beta) = v_1(t)v_2(\beta)$, where $v_1(t)$ is a time-dependent constant, and $v_2(\beta) = C_v\beta^{1/2}$. In principle, we assumed that the velocity was time independent, i.e., $v_1(t) = 1$. Figure 2 shows the best fits we found assuming isotropic ejection and constant velocity with time. The best-fitted dust mass loss rate with time (rightmost lower panel of Figure 2) reveals that a significant level of activity is already present before perihelion, increasing rapidly up to a value near 4 kg s^{-1}, and maintaining this level with just a small decrease until at least 200 days post-perihelion (last observation date). The particle sizes are confined to the 5×10^{-4} to 1 cm size range. As far as the value for constant C_v we found $C_v = 2640$ cm s^{-1}, i.e., a value of 20 cm s^{-1} for particles of 1 cm in radius. Figure 2 shows that the modeled isophotes do not reproduce adequately the brightness levels of the observations at any date, showing a much wider pattern, especially to the right side of the images, and to the left and right sides in the January 9th image. Since we could not fit the images for isotropic ejection models, the next step was to include anisotropy. To that end, we assumed an asteroid characterized by a spin axis obliquity I and a subsolar meridian at perihelion given by Φ. In this nucleus model, given an active area defined by a certain latitude box, the direction of the ejection velocity vector is computed by the formulae given by Sekanina (1981). A detailed description of the procedure is given in Moreno (2009). The longitude of the active area is not constrained because the rotation period is much shorter than the ejecta age. Thus, a trial-and-error procedure, by searching for both Φ and I in 30° steps, and for different latitude active regions, revealed that the best solutions were obtained for $I = 90°$, and $\Phi = 240°$, with emission essentially restricted to high southern latitudes. For those simulations, we assumed that 90% of the particles emitted were ejected at latitudes southward of $-50°$, while the remaining 10% were ejected in the $-50°$ to $+90°$ latitude range. Figure 3 shows that the improvement in the fits is dramatic with respect to the results given by the isotropic model, so that we can firmly conclude that P/La Sagra ejects dust anisotropically. It is interesting to note that it is the southern hemisphere the one that is oriented to the Sun at the start of the activity, with the subsolar point at $\sim -60°$ at perihelion, where activity becomes significant, and being oriented to $-90°$ at ∼120 days after perihelion (see the rightmost lower panel of

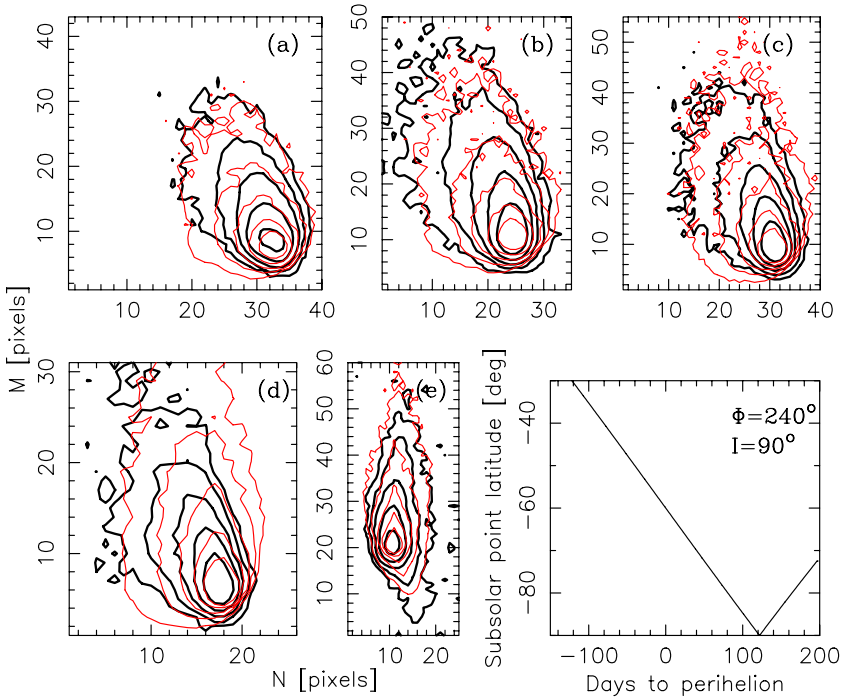

Figure 3. (a)–(e) In black thick solid lines contour plots corresponding to the observations, and in thin red lines to the anisotropic model, with ejection mostly coming from the southern hemisphere of the nucleus, with spin axis parameters $I = 90°$, $\Phi = 240°$, for the following dates (UT): (a) 2010 October 10.9; (b) 2010 October 16.0; (c) 2010 October 26.9; (d) 2010 November 4.8; (e) 2011 January 9.8. Isophotes vary in factors of two, being the innermost contour of 2×10^{-14} for panels (a) and (b), 10^{-14} for panel (c), 5×10^{-15} for panel (d), and 10^{-14} for panel (e), all expressed in solar disk intensity units. The rightmost lower panel shows the variation of the latitude of the subsolar point with time relative to perihelion.

(A color version of this figure is available in the online journal.)

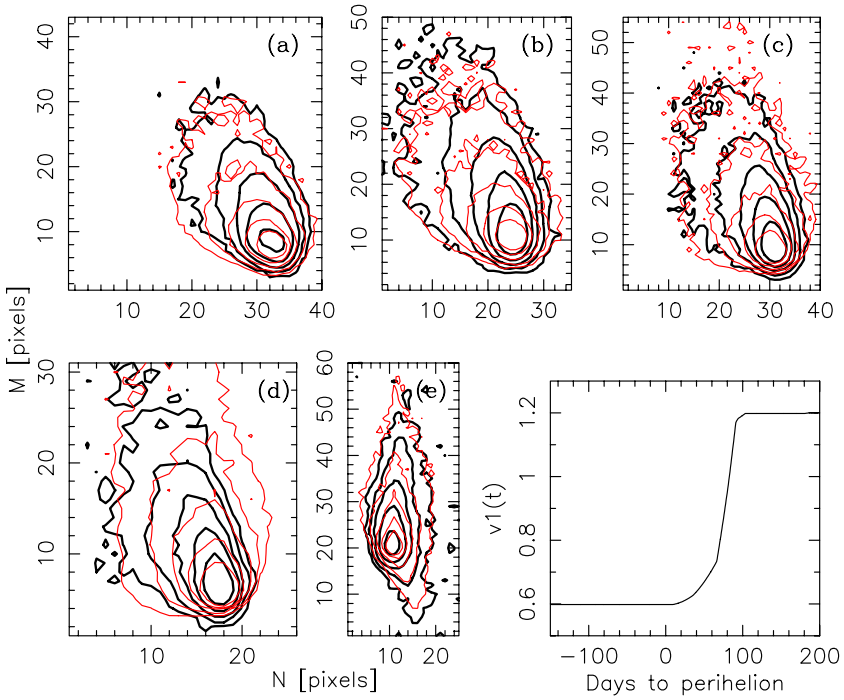

Figure 4. Results for the same anisotropic ejection model of Figure 3, but for a time-dependent ejection velocity factor $v_1(t)$, as shown in the rightmost lower panel.

(A color version of this figure is available in the online journal.)

Figure 3), suggesting a seasonal effect. The quality of the fits can be further slightly improved (Figure 4) by adopting a time-dependent ejection velocity (see the rightmost lower panel of Figure 4), with slower particles until ∼100 days post-perihelion, and faster particles later on, which, if the seasonal model were correct, would imply that the region near −90° is more active than the nearby latitude regions toward north. A seasonally driven activity on a number of MBCs has been proposed before (see, e.g., Hsieh et al. 2004; Toth 2006; Prialnik & Rosenberg 2009; Lacerda 2009; Kaluna et al. 2010). Thus, a seasonal model

on MBC 133P was first proposed by Hsieh et al. (2004), for which a large tilt angle of the spin axis has also been inferred (Prialnik & Rosenberg 2009). A seasonal heating hypothesis has also been invoked for MBC 176P/LINEAR, for which an asymmetric dust emission pattern and a high obliquity (60°) have been reported (Hsieh et al. 2011a). The current images of P/La Sagra constitute the first observations since discovery, so that little can be inferred about the cause of the event until more observations at future apparitions become available. The reported sustained activity of at least seven months is, however, incompatible with activity solely triggered by an impact, in contrary to the case of MBC (596) Scheila, for which a collision is likely the cause of the outburst (Bodewits et al. 2011; Jewitt et al. 2011; Moreno et al. 2011). The proximity to perihelion of the start of activity of P/La Sagra indicates that the activity could also be due to the sublimation of a subsurface ice reservoir by a solar radiation-driven thermal wave (Hsieh et al. 2011b), in such a way that the heliocentric distance effect could be more important than the seasonal. At present, it is not possible to favor any of these two scenarios.

5. CONCLUSIONS

We have investigated the dust environment of recently discovered MBC P/La Sagra. Observations have been performed over a three-month period shortly after discovery. By using a direct Monte Carlo modeling, we have been able to obtain the dust mass loss rate, particle ejection velocities, size distribution, and size range. These properties are typical of a sublimating ice-driven scenario, with particle terminal velocities typical of cometary activity at the heliocentric distances at which the object was observed. The onset of activity is constrained to occur shortly before perihelion, reaching rapidly a level of sustained activity of 3–4 kg s^{-1} lasting at least seven months. Isotropic ejection models are unable to fit the isophotes of the observed images at the different dates, that are otherwise very well fitted with anisotropic ejection models, with particle ejection coming mostly from high southern latitudes, for an obliquity of $I = 90°$, and an argument of the subsolar meridian at perihelion of $\Phi = 240°$. These parameters imply that the south polar regions are the most exposed to solar radiation at the onset time and afterward, indicating a possible seasonal nature of the event, like in the cases of MBCs 133P or 176P (Hsieh et al. 2004, 2011a). However, the proximity to perihelion of the onset indicates that the heliocentric distance effect could also be playing a role. More observations of this object are needed in order to determine the origin and the nature of the activity.

This Letter is partially based on observations made with the Italian Telescopio Nazionale Galileo (TNG) operated on the island of La Palma by the Fundación Galileo Galilei of the INAF (Istituto Nazionale di Astrofisica) at the Spanish Observatorio del Roque de los Muchachos of the Instituto de Astrofísica de Canarias; on the William Herschel Telescope (WHT) operated on the island of La Palma by the Isaac Newton Group in the Spanish Observatorio del Roque de los Muchachos of the Instituto de Astrofísica de Canarias; on observations made with the 2.2 m telescope of the Centro Astronómico Hispano-Alemán at Calar Alto, operated jointly by the Max-Planck-Institut für Astronomie and the Instituto de Astrofísica de Andalucía (CSIC); on observations made with the Nordic Optical Telescope (NOT), operated on the island of La Palma jointly by Denmark, Finland, Iceland, Norway, and Sweden, in the Spanish Observatorio del Roque de los Muchachos of the Instituto de Astrofisica de Canarias. The data presented here were obtained in part with ALFOSC at NOT, which is provided by the Instituto de Astrofísica de Andalucía (IAA) under a joint agreement with the University of Copenhagen and NOTSA.

This work was supported by contracts AYA2007-63670, AYA2008-01720E, AYA2009-08190, AYA2009-08011, and FQM-03837 and FQM-4555 (Proyectos de Excelencia, Junta de Andalucía). J.L., V.A.-L., and B.A.G. gratefully acknowledge support from the spanish "Ministerio de Ciencia e Innovación" project AYA2008-06202-C03-02. J.L.O. gratefully acknowledges support from the spanish "Ministerio de Ciencia e Innovación" project AYA2008-06202-C03-01.

REFERENCES

Bertini, I. 2011, Planet. Space Sci., 59, 365
Bodewits, D., Kelley, M. S., Li, J. Y., et al. 2011, ApJ, 733, L3
Burns, J. A., Lamy, P. L., & Soter, S. 1979, Icarus, 40, 1
Finson, M., & Probstein, R. 1968, ApJ, 154, 327
Fulle, M. 1989, A&A, 217, 283
Fulle, M., Colangeli, L., Agarwal, J., et al. 2010, A&A, 522, 63
Hsieh, H. H., Ishiguro, M., Lacerda, P., & Jewitt, D. 2011a, AJ, 142, 29
Hsieh, H. H., & Jewitt, D. 2006, Science, 312, 561
Hsieh, H. H., Jewitt, D., & Fernández, Y. 2004, AJ, 127, 2997
Hsieh, H. H., Jewitt, D., & Ishiguro, M. 2009, AJ, 137, 157
Hsieh, H. H., Meech, K., & Pittichova, J. 2011b, ApJ, 736, L18
Jewitt, D., Weaver, H., Mutchler, M., Larson, S., & Agarwal, J. 2011, ApJ, 733, L4
Jockers, K. 1997, Earth Moon Planets, 79, 221
Kaluna, H. M., Meech, K. J., Pittichova, J., et al. 2010, in Astrobiology Science Conf. 2010: Evolution and Life—Surviving Catastrophes and Extremes on Earth and Beyond, LPI Contrib. No. 1538, 5559
Lacerda, P. 2009, in European Planetary Science Congress 2009, 815
Larson, S. M. 2010, IAU Circ., 9188, 1
Monet, D. G., Levine, S. E., Canzian, B., et al. 2003, AJ, 125, 984
Moreno, F. 2009, ApJS, 183, 33
Moreno, F., Licandro, J., Ortiz, J. L., et al. 2011, ApJ, 738, 130
Moreno, F., Licandro, J., Tozzi, G.-P., et al. 2010, ApJ, 718, L132
Nomen, J., Birtwhistle, P., Holmes, R., Foglia, S., & Scotti, J. V. 2010, CBET, 2459, 1
Prialnik, D., & Rosenberg, E. D. 2009, MNRAS, 399, L79
Sekanina, Z. 1981, Annu. Rev. Earth Planet. Sci., 9, 113
Toth, I. 2006, A&A, 446, 333